PHYSICAL REVIEW D **77,** 091104(R) (2008)

Searches for the decays $B^0 \to l^\pm \tau^\mp$ and $B^+ \to l^+ \nu$ ($l = e, \mu$) using hadronic tag reconstruction

B. Aubert,[1] M. Bona,[1] Y. Karyotakis,[1] J. P. Lees,[1] V. Poireau,[1] X. Prudent,[1] V. Tisserand,[1] A. Zghiche,[1] J. Garra Tico,[2] E. Grauges,[2] L. Lopez,[3] A. Palano,[3] M. Pappagallo,[3] G. Eigen,[4] B. Stugu,[4] L. Sun,[4] G. S. Abrams,[5] M. Battaglia,[5] D. N. Brown,[5] J. Button-Shafer,[5] R. N. Cahn,[5] R. G. Jacobsen,[5] J. A. Kadyk,[5] L. T. Kerth,[5] Yu. G. Kolomensky,[5] G. Kukartsev,[5] D. Lopes Pegna,[5] G. Lynch,[5] I. L. Osipenkov,[5] M. T. Ronan,[5,*] K. Tackmann,[5] T. Tanabe,[5] W. A. Wenzel,[5] P. del Amo Sanchez,[6] C. M. Hawkes,[6] N. Soni,[6] A. T. Watson,[6] H. Koch,[7] T. Schroeder,[7] D. Walker,[8] D. J. Asgeirsson,[9] T. Cuhadar-Donszelmann,[9] B. G. Fulsom,[9] C. Hearty,[9] T. S. Mattison,[9] J. A. McKenna,[9] M. Barrett,[10] A. Khan,[10] M. Saleem,[10] L. Teodorescu,[10] V. E. Blinov,[11] A. D. Bukin,[11] A. R. Buzykaev,[11] V. P. Druzhinin,[11] V. B. Golubev,[11] A. P. Onuchin,[11] S. I. Serednyakov,[11] Yu. I. Skovpen,[11] E. P. Solodov,[11] K. Yu. Todyshev,[11] M. Bondioli,[12] S. Curry,[12] I. Eschrich,[12] D. Kirkby,[12] A. J. Lankford,[12] P. Lund,[12] M. Mandelkern,[12] E. C. Martin,[12] D. P. Stoker,[12] S. Abachi,[13] C. Buchanan,[13] J. W. Gary,[14] F. Liu,[14] O. Long,[14] B. C. Shen,[14,*] G. M. Vitug,[14] L. Zhang,[14] H. P. Paar,[15] S. Rahatlou,[15] V. Sharma,[15] C. Campagnari,[16] T. M. Hong,[16] D. Kovalskyi,[16] J. D. Richman,[16] T. W. Beck,[17] A. M. Eisner,[17] C. J. Flacco,[17] C. A. Heusch,[17] J. Kroseberg,[17] W. S. Lockman,[17] T. Schalk,[17] B. A. Schumm,[17] A. Seiden,[17] M. G. Wilson,[17] L. O. Winstrom,[17] E. Chen,[18] C. H. Cheng,[18] D. A. Doll,[18] B. Echenard,[18] F. Fang,[18] D. G. Hitlin,[18] I. Narsky,[18] T. Piatenko,[18] F. C. Porter,[18] R. Andreassen,[19] G. Mancinelli,[19] B. T. Meadows,[19] K. Mishra,[19] M. D. Sokoloff,[19] F. Blanc,[20] P. C. Bloom,[20] W. T. Ford,[20] J. F. Hirschauer,[20] A. Kreisel,[20] M. Nagel,[20] U. Nauenberg,[20] A. Olivas,[20] J. G. Smith,[20] K. A. Ulmer,[20] S. R. Wagner,[20] R. Ayad,[21,+] A. M. Gabareen,[21] A. Soffer,[21,‡] W. H. Toki,[21] R. J. Wilson,[21] D. D. Altenburg,[22] E. Feltresi,[22] A. Hauke,[22] H. Jasper,[22] J. Merkel,[22] A. Petzold,[22] B. Spaan,[22] K. Wacker,[22] V. Klose,[23] M. J. Kobel,[23] H. M. Lacker,[23] W. F. Mader,[23] R. Nogowski,[23] J. Schubert,[23] K. R. Schubert,[23] R. Schwierz,[23] J. E. Sundermann,[23] A. Volk,[23] D. Bernard,[24] G. R. Bonneaud,[24] E. Latour,[24] V. Lombardo,[24] Ch. Thiebaux,[24] M. Verderi,[24] P. J. Clark,[25] W. Gradl,[25] S. Playfer,[25] A. I. Robertson,[25] J. E. Watson,[25] M. Andreotti,[26] D. Bettoni,[26] C. Bozzi,[26] R. Calabrese,[26] A. Cecchi,[26] G. Cibinetto,[26] P. Franchini,[26] E. Luppi,[26] M. Negrini,[26] A. Petrella,[26] L. Piemontese,[26] E. Prencipe,[26] V. Santoro,[26] F. Anulli,[27] R. Baldini-Ferroli,[27] A. Calcaterra,[27] R. de Sangro,[27] G. Finocchiaro,[27] S. Pacetti,[27] P. Patteri,[27] I. M. Peruzzi,[27,§] M. Piccolo,[27] M. Rama,[27] A. Zallo,[27] A. Buzzo,[28] R. Contri,[28] M. Lo Vetere,[28] M. M. Macri,[28] M. R. Monge,[28] S. Passaggio,[28] C. Patrignani,[28] E. Robutti,[28] A. Santroni,[28] S. Tosi,[28] K. S. Chaisanguanthum,[29] M. Morii,[29] R. S. Dubitzky,[30] J. Marks,[30] S. Schenk,[30] U. Uwer,[30] D. J. Bard,[31] P. D. Dauncey,[31] J. A. Nash,[31] W. Panduro Vazquez,[31] M. Tibbetts,[31] P. K. Behera,[32] X. Chai,[32] M. J. Charles,[32] U. Mallik,[32] J. Cochran,[33] H. B. Crawley,[33] L. Dong,[33] V. Eyges,[33] W. T. Meyer,[33] S. Prell,[33] E. I. Rosenberg,[33] A. E. Rubin,[33] Y. Y. Gao,[34] A. V. Gritsan,[34] Z. J. Guo,[34] C. K. Lae,[34] A. G. Denig,[35] M. Fritsch,[35] G. Schott,[35] N. Arnaud,[36] J. Béquilleux,[36] A. D'Orazio,[36] M. Davier,[36] J. Firmino da Costa,[36] G. Grosdidier,[36] A. Höcker,[36] V. Lepeltier,[36] F. Le Diberder,[36] A. M. Lutz,[36] S. Pruvot,[36] P. Roudeau,[36] M. H. Schune,[36] J. Serrano,[36] V. Sordini,[36] A. Stocchi,[36] W. F. Wang,[36] G. Wormser,[36] D. J. Lange,[37] D. M. Wright,[37] I. Bingham,[38] J. P. Burke,[38] C. A. Chavez,[38] J. R. Fry,[38] E. Gabathuler,[38] R. Gamet,[38] D. E. Hutchcroft,[38] D. J. Payne,[38] C. Touramanis,[38] A. J. Bevan,[39] K. A. George,[39] F. Di Lodovico,[39] R. Sacco,[39] G. Cowan,[40] H. U. Flaecher,[40] D. A. Hopkins,[40] S. Paramesvaran,[40] F. Salvatore,[40] A. C. Wren,[40] D. N. Brown,[41] C. L. Davis,[41] N. R. Barlow,[42] R. J. Barlow,[42] Y. M. Chia,[42] C. L. Edgar,[42] G. D. Lafferty,[42] T. J. West,[42] J. I. Yi,[42] J. Anderson,[43] C. Chen,[43] A. Jawahery,[43] D. A. Roberts,[43] G. Simi,[43] J. M. Tuggle,[43] C. Dallapiccola,[44] S. S. Hertzbach,[44] X. Li,[44] T. B. Moore,[44] E. Salvati,[44] S. Saremi,[44] R. Cowan,[45] D. Dujmic,[45] P. H. Fisher,[45] K. Koeneke,[45] G. Sciolla,[45] M. Spitznagel,[45] F. Taylor,[45] R. K. Yamamoto,[45] M. Zhao,[45] M. Klemetti,[46] S. E. Mclachlin,[46,*] P. M. Patel,[46] S. H. Robertson,[46] A. Lazzaro,[47] F. Palombo,[47] J. M. Bauer,[48] L. Cremaldi,[48] V. Eschenburg,[48] R. Godang,[48] R. Kroeger,[48] D. A. Sanders,[48] D. J. Summers,[48] H. W. Zhao,[48] S. Brunet,[49] D. Côté,[49] M. Simard,[49] P. Taras,[49] F. B. Viaud,[49] H. Nicholson,[50] G. De Nardo,[51] L. Lista,[51] D. Monorchio,[51] C. Sciacca,[51] M. A. Baak,[52] G. Raven,[52] H. L. Snoek,[52] C. P. Jessop,[53] K. J. Knoepfel,[53] J. M. LoSecco,[53] G. Benelli,[54] L. A. Corwin,[54] K. Honscheid,[54] H. Kagan,[54] R. Kass,[54] J. P. Morris,[54] A. M. Rahimi,[54] J. J. Regensburger,[54] S. J. Sekula,[54] Q. K. Wong,[54] N. L. Blount,[55] J. Brau,[55] R. Frey,[55] O. Igonkina,[55] J. A. Kolb,[55] M. Lu,[55] R. Rahmat,[55] N. B. Sinev,[55] D. Strom,[55] J. Strube,[55] E. Torrence,[55] G. Castelli,[56] N. Gagliardi,[56] A. Gaz,[56] M. Margoni,[56] M. Morandin,[56] A. Pompili,[56] M. Posocco,[56] M. Rotondo,[56] F. Simonetto,[56] R. Stroili,[56] C. Voci,[56] E. Ben-Haim,[57] H. Briand,[57] G. Calderini,[57] J. Chauveau,[57] P. David,[57] L. Del Buono,[57] Ch. de la Vaissière,[57] O. Hamon,[57] Ph. Leruste,[57] J. Malclès,[57] J. Ocariz,[57] A. Perez,[57] J. Prendki,[57] L. Gladney,[58] M. Biasini,[59] R. Covarelli,[59] E. Manoni,[59] C. Angelini,[60] G. Batignani,[60] S. Bettarini,[60] M. Carpinelli,[60,‖] R. Cenci,[60] A. Cervelli,[60] F. Forti,[60] M. A. Giorgi,[60] A. Lusiani,[60] G. Marchiori,[60] M. A. Mazur,[60] M. Morganti,[60] N. Neri,[60] E. Paoloni,[60] G. Rizzo,[60] J. J. Walsh,[60] J. Biesiada,[61] Y. P. Lau,[61] C. Lu,[61]

J. Olsen,[61] A. J. S. Smith,[61] A. V. Telnov,[61] E. Baracchini,[62] G. Cavoto,[62] D. del Re,[62] E. Di Marco,[62] R. Faccini,[62] F. Ferrarotto,[62] F. Ferroni,[62] M. Gaspero,[62] P. D. Jackson,[62] M. A. Mazzoni,[62] S. Morganti,[62] G. Piredda,[62] F. Polci,[62] F. Renga,[62] C. Voena,[62] M. Ebert,[63] T. Hartmann,[63] H. Schröder,[63] R. Waldi,[63] T. Adye,[64] B. Franek,[64] E. O. Olaiya,[64] W. Roethel,[64] F. F. Wilson,[64] S. Emery,[65] M. Escalier,[65] A. Gaidot,[65] S. F. Ganzhur,[65] G. Hamel de Monchenault,[65] W. Kozanecki,[65] G. Vasseur,[65] Ch. Yèche,[65] M. Zito,[65] X. R. Chen,[66] H. Liu,[66] W. Park,[66] M. V. Purohit,[66] R. M. White,[66] J. R. Wilson,[66] M. T. Allen,[67] D. Aston,[67] R. Bartoldus,[67] P. Bechtle,[67] R. Claus,[67] J. P. Coleman,[67] M. R. Convery,[67] J. C. Dingfelder,[67] J. Dorfan,[67] G. P. Dubois-Felsmann,[67] W. Dunwoodie,[67] R. C. Field,[67] T. Glanzman,[67] S. J. Gowdy,[67] M. T. Graham,[67] P. Grenier,[67] C. Hast,[67] W. R. Innes,[67] J. Kaminski,[67] M. H. Kelsey,[67] H. Kim,[67] P. Kim,[67] M. L. Kocian,[67] D. W. G. S. Leith,[67] S. Li,[67] S. Luitz,[67] V. Luth,[67] H. L. Lynch,[67] D. B. MacFarlane,[67] H. Marsiske,[67] R. Messner,[67] D. R. Muller,[67] S. Nelson,[67] C. P. O'Grady,[67] I. Ofte,[67] A. Perazzo,[67] M. Perl,[67] B. N. Ratcliff,[67] A. Roodman,[67] A. A. Salnikov,[67] R. H. Schindler,[67] J. Schwiening,[67] A. Snyder,[67] D. Su,[67] M. K. Sullivan,[67] K. Suzuki,[67] S. K. Swain,[67] J. M. Thompson,[67] J. Va'vra,[67] A. P. Wagner,[67] M. Weaver,[67] W. J. Wisniewski,[67] M. Wittgen,[67] D. H. Wright,[67] H. W. Wulsin,[67] A. K. Yarritu,[67] K. Yi,[67] C. C. Young,[67] V. Ziegler,[67] P. R. Burchat,[68] A. J. Edwards,[68] S. A. Majewski,[68] T. S. Miyashita,[68] B. A. Petersen,[68] L. Wilden,[68] S. Ahmed,[69] M. S. Alam,[69] R. Bula,[69] J. A. Ernst,[69] B. Pan,[69] M. A. Saeed,[69] S. B. Zain,[69] S. M. Spanier,[70] B. J. Wogsland,[70] R. Eckmann,[71] J. L. Ritchie,[71] A. M. Ruland,[71] C. J. Schilling,[71] R. F. Schwitters,[71] J. M. Izen,[72] X. C. Lou,[72] S. Ye,[72] F. Bianchi,[73] D. Gamba,[73] M. Pelliccioni,[73] M. Bomben,[74] L. Bosisio,[74] C. Cartaro,[74] F. Cossutti,[74] G. Della Ricca,[74] L. Lanceri,[74] L. Vitale,[74] V. Azzolini,[75] N. Lopez-March,[75] F. Martinez-Vidal,[75] D. A. Milanes,[75] A. Oyanguren,[75] J. Albert,[76] Sw. Banerjee,[76] B. Bhuyan,[76] K. Hamano,[76] R. Kowalewski,[76] I. M. Nugent,[76] J. M. Roney,[76] R. J. Sobie,[76] P. F. Harrison,[77] J. Ilic,[77] T. E. Latham,[77] G. B. Mohanty,[77] H. R. Band,[78] X. Chen,[78] S. Dasu,[78] K. T. Flood,[78] J. J. Hollar,[78] P. E. Kutter,[78] Y. Pan,[78] M. Pierini,[78] R. Prepost,[78] S. L. Wu,[78] and H. Neal[79]

(*BABAR* Collaboration)

[1]*Laboratoire de Physique des Particules, IN2P3/CNRS et Université de Savoie, F-74941 Annecy-Le-Vieux, France*
[2]*Universitat de Barcelona, Facultat de Fisica, Departament ECM, E-08028 Barcelona, Spain*
[3]*Università di Bari, Dipartimento di Fisica and INFN, I-70126 Bari, Italy*
[4]*University of Bergen, Institute of Physics, N-5007 Bergen, Norway*
[5]*Lawrence Berkeley National Laboratory and University of California, Berkeley, California 94720, USA*
[6]*University of Birmingham, Birmingham, B15 2TT, United Kingdom*
[7]*Ruhr Universität Bochum, Institut für Experimentalphysik 1, D-44780 Bochum, Germany*
[8]*University of Bristol, Bristol BS8 1TL, United Kingdom*
[9]*University of British Columbia, Vancouver, British Columbia, Canada V6T 1Z1*
[10]*Brunel University, Uxbridge, Middlesex UB8 3PH, United Kingdom*
[11]*Budker Institute of Nuclear Physics, Novosibirsk 630090, Russia*
[12]*University of California at Irvine, Irvine, California 92697, USA*
[13]*University of California at Los Angeles, Los Angeles, California 90024, USA*
[14]*University of California at Riverside, Riverside, California 92521, USA*
[15]*University of California at San Diego, La Jolla, California 92093, USA*
[16]*University of California at Santa Barbara, Santa Barbara, California 93106, USA*
[17]*University of California at Santa Cruz, Institute for Particle Physics, Santa Cruz, California 95064, USA*
[18]*California Institute of Technology, Pasadena, California 91125, USA*
[19]*University of Cincinnati, Cincinnati, Ohio 45221, USA*
[20]*University of Colorado, Boulder, Colorado 80309, USA*
[21]*Colorado State University, Fort Collins, Colorado 80523, USA*
[22]*Universität Dortmund, Institut für Physik, D-44221 Dortmund, Germany*
[23]*Technische Universität Dresden, Institut für Kern- und Teilchenphysik, D-01062 Dresden, Germany*
[24]*Laboratoire Leprince-Ringuet, CNRS/IN2P3, Ecole Polytechnique, F-91128 Palaiseau, France*
[25]*University of Edinburgh, Edinburgh EH9 3JZ, United Kingdom*
[26]*Università di Ferrara, Dipartimento di Fisica and INFN, I-44100 Ferrara, Italy*
[27]*Laboratori Nazionali di Frascati dell'INFN, I-00044 Frascati, Italy*
[28]*Università di Genova, Dipartimento di Fisica and INFN, I-16146 Genova, Italy*
[29]*Harvard University, Cambridge, Massachusetts 02138, USA*
[30]*Universität Heidelberg, Physikalisches Institut, Philosophenweg 12, D-69120 Heidelberg, Germany*
[31]*Imperial College London, London, SW7 2AZ, United Kingdom*
[32]*University of Iowa, Iowa City, Iowa 52242, USA*

[33]*Iowa State University, Ames, Iowa 50011-3160, USA*
[34]*Johns Hopkins University, Baltimore, Maryland 21218, USA*
[35]*Universität Karlsruhe, Institut für Experimentelle Kernphysik, D-76021 Karlsruhe, Germany*
[36]*Laboratoire de l'Accélérateur Linéaire, IN2P3/CNRS et Université Paris-Sud 11, Centre Scientifique d'Orsay, B. P. 34, F-91898 ORSAY Cedex, France*
[37]*Lawrence Livermore National Laboratory, Livermore, California 94550, USA*
[38]*University of Liverpool, Liverpool L69 7ZE, United Kingdom*
[39]*Queen Mary, University of London, E1 4NS, United Kingdom*
[40]*University of London, Royal Holloway and Bedford New College, Egham, Surrey TW20 0EX, United Kingdom*
[41]*University of Louisville, Louisville, Kentucky 40292, USA*
[42]*University of Manchester, Manchester M13 9PL, United Kingdom*
[43]*University of Maryland, College Park, Maryland 20742, USA*
[44]*University of Massachusetts, Amherst, Massachusetts 01003, USA*
[45]*Massachusetts Institute of Technology, Laboratory for Nuclear Science, Cambridge, Massachusetts 02139, USA*
[46]*McGill University, Montréal, Québec, Canada H3A 2T8*
[47]*Università di Milano, Dipartimento di Fisica and INFN, I-20133 Milano, Italy*
[48]*University of Mississippi, University, Mississippi 38677, USA*
[49]*Université de Montréal, Physique des Particules, Montréal, Québec, Canada H3C 3J7*
[50]*Mount Holyoke College, South Hadley, Massachusetts 01075, USA*
[51]*Università di Napoli Federico II, Dipartimento di Scienze Fisiche and INFN, I-80126, Napoli, Italy*
[52]*NIKHEF, National Institute for Nuclear Physics and High Energy Physics, NL-1009 DB Amsterdam, The Netherlands*
[53]*University of Notre Dame, Notre Dame, Indiana 46556, USA*
[54]*Ohio State University, Columbus, Ohio 43210, USA*
[55]*University of Oregon, Eugene, Oregon 97403, USA*
[56]*Università di Padova, Dipartimento di Fisica and INFN, I-35131 Padova, Italy*
[57]*Laboratoire de Physique Nucléaire et de Hautes Energies, IN2P3/CNRS, Université Pierre et Marie Curie-Paris6, Université Denis Diderot-Paris7, F-75252 Paris, France*
[58]*University of Pennsylvania, Philadelphia, Pennsylvania 19104, USA*
[59]*Università di Perugia, Dipartimento di Fisica and INFN, I-06100 Perugia, Italy*
[60]*Università di Pisa, Dipartimento di Fisica, Scuola Normale Superiore and INFN, I-56127 Pisa, Italy*
[61]*Princeton University, Princeton, New Jersey 08544, USA*
[62]*Università di Roma La Sapienza, Dipartimento di Fisica and INFN, I-00185 Roma, Italy*
[63]*Universität Rostock, D-18051 Rostock, Germany*
[64]*Rutherford Appleton Laboratory, Chilton, Didcot, Oxon, OX11 0QX, United Kingdom*
[65]*DSM/Dapnia, CEA/Saclay, F-91191 Gif-sur-Yvette, France*
[66]*University of South Carolina, Columbia, South Carolina 29208, USA*
[67]*Stanford Linear Accelerator Center, Stanford, California 94309, USA*
[68]*Stanford University, Stanford, California 94305-4060, USA*
[69]*State University of New York, Albany, New York 12222, USA*
[70]*University of Tennessee, Knoxville, Tennessee 37996, USA*
[71]*University of Texas at Austin, Austin, Texas 78712, USA*
[72]*University of Texas at Dallas, Richardson, Texas 75083, USA*
[73]*Università di Torino, Dipartimento di Fisica Sperimentale and INFN, I-10125 Torino, Italy*
[74]*Università di Trieste, Dipartimento di Fisica and INFN, I-34127 Trieste, Italy*
[75]*IFIC, Universitat de Valencia-CSIC, E-46071 Valencia, Spain*
[76]*University of Victoria, Victoria, British Columbia, Canada V8W 3P6*
[77]*Department of Physics, University of Warwick, Coventry CV4 7AL, United Kingdom*
[78]*University of Wisconsin, Madison, Wisconsin 53706, USA*
[79]*Yale University, New Haven, Connecticut 06511, USA*

(Received 7 January 2008; published 21 May 2008)

We present searches for the leptonic decays $B^+ \to \ell^+ \nu$ and the lepton flavor violating decays $B^0 \to \ell^\pm \tau^\mp$, where $\ell = e, \mu$, with data collected by the *BABAR* experiment at SLAC. This search demonstrates a novel technique in which we fully reconstruct the accompanying $\bar{B}$ in $\Upsilon(4S) \to B\bar{B}$ events, and look for a monoenergetic lepton from the signal B decay. The signal yield is extracted from a fit to the signal lepton candidate momentum distribution in the signal B rest frame. Using a data sample of approximately 378×10^6 $B\bar{B}$ pairs ($342\ \mathrm{fb}^{-1}$), we find no evidence of signal in any of the decay modes. Branching fraction upper limits of $\mathcal{B}(B^+ \to e^+ \nu) < 5.2 \times 10^{-6}$, $\mathcal{B}(B^+ \to \mu^+ \nu) < 5.6 \times 10^{-6}$, $\mathcal{B}(B^0 \to e^+ \tau^-) < 2.8 \times 10^{-5}$ and $\mathcal{B}(B^0 \to \mu^+ \tau^-) < 2.2 \times 10^{-5}$, are obtained at 90% confidence level.

DOI: 10.1103/PhysRevD.77.091104 PACS numbers: 13.25.Hw, 12.15.Hh, 11.30.Er

In this paper, we present searches for the decays $B^+ \to \ell^+ \nu$ and the lepton flavor violating decays $B^0 \to \ell^\pm \tau^\mp$, where $\ell = e, \mu$ [1], using a technique in which the accompanying B in the event is exclusively reconstructed. This method has not previously been used for searches for these modes and, although statistically limited with the present *BABAR* data sample, shows promise for future studies at, for example, a high luminosity Super B factory [2]. While the former decay modes are allowed in the standard model (SM) and the latter are not, both are potentially sensitive to new physics (NP) effects, such as contributions by neutral and charged non-SM Higgs [3,4].

Searches for rare B decays with neutrinos in the final state are challenging due to the limited availability of kinematic constraints. However, purely leptonic B decays involving an electron or a muon have a clear experimental signature in the form of a high momentum lepton. Combined with clean theoretical predictions due to the lack of QCD contributions in the final state, such leptonic B decays present an ideal place to test the SM against NP models.

In the SM, $B^+ \to \ell^+ \nu$ decays proceed via an annihilation of $\bar{b}$ and u quarks into a virtual W^+ boson. In the SM the branching fraction for this type of decay is given by [5]:

$$\mathcal{B}(B^+ \to \ell^+ \nu_\ell) = \frac{G_F^2 m_B m_l^2}{8\pi}\left(1 - \frac{m_l^2}{m_B^2}\right) f_B^2 |V_{ub}|^2 \tau_B, \quad (1)$$

where G_F is the Fermi coupling constant, m_l is the lepton mass and m_B, τ_B, and f_B are the mass, lifetime and decay constant for the B meson. The Cabibbo-Kobayashi-Maskawa matrix element $|V_{ub}|$ describes the transition from b to u quarks [6]. Within the SM, a determination of any one of the leptonic branching fractions represents a determination of the product $|V_{ub}| \cdot f_B$, which can be directly compared with determinations from lattice calculations, B-mixing, and semileptonic decay measurements [7,8]. As seen in Eq. (1), the decay rates are proportional to m_l^2, resulting in SM predictions for the μ and e modes which are suppressed by factors on the order of 250 and 10^7, respectively, compared with the τ mode. Taking the branching fraction $\mathcal{B}(B^+ \to \tau^+ \nu_\tau) = (1.31 \pm 0.48) \times 10^{-4}$ from the combination of recent *BABAR* and BELLE results [9,10] implies $\mathcal{B}_{SM}(B^+ \to \mu^+ \nu_\mu) \sim 5.2 \times 10^{-7}$ and $\mathcal{B}_{SM}(B^+ \to e^+ \nu_e) \sim 1.2 \times 10^{-11}$. New physics contributions to these processes can enhance or suppress the decay rates compared to the SM, and may either preserve or violate the relative rates of the three leptonic modes depending on the particular NP model [3,11]. Thus, the e and μ modes become particularly interesting in light of recent evidence for the $B^+ \to \tau^+ \nu_\tau$ decay mode. In addition, the observed discrepancy of the $D_s^+ \to \tau^+ \nu_\tau$ decay constant from its lattice QCD prediction [12,13] gives hints of new physics that may also contribute to the leptonic B decay modes. Currently, the most stringent published limits on $B^+ \to \ell^+ \nu$ are from the BELLE collaboration with $\mathcal{B}(B^+ \to e^+ \nu) < 9.8 \times 10^{-7}$ and $\mathcal{B}(B^+ \to \mu^+ \nu) < 1.7 \times 10^{-6}$ [14]. Earlier studies by CLEO and *BABAR* collaborations are also available [15,16].

The lepton-flavor-violating (LFV) leptonic B decays, such as $B^0 \to \ell^+ \tau^-$, are forbidden in the SM in the absence of nonzero neutrino masses, but can occur via one-loop diagrams if neutrino oscillations are included. The rates of such processes, however, would be substantially below current or anticipated future experimental sensitivities. On the other hand, many models of physics beyond the SM, in particular, supersymmetric seesaw models [4], predict dramatically higher rates for these decays. In the case of Higgs-mediated LFV processes, couplings to heavier leptons are favored, making $B^0 \to \ell^+ \tau^-$ particularly interesting. In the general flavor-universal MSSM, the branching fractions allowed for $B^0 \to \ell^+ \tau^-$ are $\sim 2 \times 10^{-10}$ [4]. Such decays could be within the reach of a Super B factory with a data sample of 50 to 75 ab^{-1}. The current best experimental limits on the branching fractions for these two decays are $\mathcal{B}(B^0 \to e^+ \tau^-) < 1.1 \times 10^{-4}$ and $\mathcal{B}(B^0 \to \mu^+ \tau^-) < 3.8 \times 10^{-5}$, set by the CLEO collaboration with 10 fb^{-1} of data [17].

The searches described in this work are based on a data sample of approximately 378×10^6 $B\bar{B}$ pairs, corresponding to an integrated luminosity of 342 fb^{-1} collected at the $\Upsilon(4S)$ resonance by the *BABAR* detector at the PEP-II asymmetric e^+e^- storage ring. Reconstructing the accompanying B meson in specific hadronic modes prior to the signal selection allows the missing momentum vector of the neutrino(s) to be fully determined. The resulting increase in the energy resolution and the ability to infer the signal B meson rest frame provide the extra kinematic handles that permit signal events to be cleanly distinguished from the background. Previous B factory searches for $B^+ \to \ell^+ \nu$ and $B^0 \to \ell^+ \tau^-$ have used an inclusive method in which the accompanying B is not explicitly reconstructed. This results in an order of magnitude gain in the selection efficiency, which with the current level of luminosity allows more stringent limits. However, due to the very small background achievable with the exclusive method, the two methods have a comparable sensitivity for the observation of a statistically significant signal. The method described in this paper will be the preferred approach for the high-precision studies of leptonic B decays. In particular, the SM predicted decay rate for $B^+ \to \mu^+ \nu$ is well within the reach of a high luminosity B factory.

Charged-particle tracking and dE/dx measurements for particle identification are provided by a five-layer double-sided silicon vertex tracker and a 40-layer drift chamber contained within the magnetic field of a 1.5 T superconducting solenoid. A ring-imaging Cherenkov detector provides efficient particle identification. The energies of neutral particles are measured with an electromagnetic calorimeter (EMC) consisting of 6580 CsI(Tl) crystals arrayed in a cylindrical barrel and in a forward endcap.

Muon identification is provided by resistive plate chambers (partially replaced by limited streamer tubes for a subset of the data that is used in this analysis) interleaved with the passive material comprising the solenoid magnetic flux return. Signal efficiencies and background rates are estimated using a Monte Carlo (MC) simulation of the *BABAR* detector based on GEANT4 [18]. The *BABAR* detector is described in detail in Ref. [19].

Reconstructed charged tracks are assigned a particle hypothesis based on information from detector subsystems. K_s^0 candidates are selected by combining oppositely charged π candidates and requiring that the $\pi^+\pi^-$ invariant mass satisfies $0.47\ \text{GeV}/c^2 < m_{\pi^+\pi^-} < 0.52\ \text{GeV}/c^2$. π^0 candidates are obtained from the combination of EMC clusters with no associated tracks, each with a $\Upsilon(4S)$ center-of-mass (CM) rest frame energy greater than 20 MeV, for which the $\gamma\gamma$ invariant mass satisfies $115\ \text{MeV}/c^2 < m_{\gamma\gamma} < 150\ \text{MeV}/c^2$.

Over 96% of the time, the $\Upsilon(4S)$ resonance decays into a pair of B mesons [20]. Since the CM energy is precisely known at PEP-II, exclusive reconstruction of one of the two B mesons, which we denote B_{tag}, fully determines the momentum four-vector of the other B meson in the event. Charged and neutral B meson candidates are reconstructed in hadronic final states of the form $B \to D^{(*)}X_{\text{had}}$ [21]. The reconstruction procedure begins with a $D^{(*)0}$ or $D^{(*)\pm}$ seed, to which charged and neutral pions and kaons (which form the X_{had} system) are then added. The combination of the $D^{(*)}$ and X_{had} with the lowest value of $\Delta E = |E_B - E_{\text{beam}}|$ that satisfies the condition $\Delta E < 0.2$ GeV is chosen as the B_{tag} candidate, where E_B is the energy of the reconstructed B meson and E_{beam} is the beam energy, both evaluated in the CM frame. We reconstruct D^{*+} in the $D^+\pi^0$ and $D^0\pi^+$ channels, and D^{*0} in the $D^0\pi^0$ and $D^0\gamma$ channels. The D^+ is reconstructed in the modes $K^-\pi^+\pi^+$, $K_s^0\pi^+$, $K_s^0\pi^+\pi^0$, $K^-\pi^+\pi^+\pi^0$, and $K_s^0\pi^+\pi^+\pi^-$. For D^0 we consider the modes $K^-\pi^+$, $K^-\pi^+\pi^0$, $K^-\pi^+\pi^+\pi^-$, and $K_s^0\pi^+\pi^-$.

Although multiple $D^{(*)}X_{\text{had}}$ combinations may be present in a single event, this procedure permits, at most, a single B_{tag} candidate to be retained in any given event. For the B_{tag} candidate, we define the energy substituted mass, $m_{\text{ES}} = \sqrt{E_{\text{beam}}^2 - \vec{p}_B^{\,2}}$, where $\vec{p}_B$ is the momentum of the B_{tag} candidate in the CM frame. B_{tag} candidates that are correctly reconstructed peak in m_{ES} near the nominal B meson mass, while incorrectly reconstructed B_{tag} candidates produce a combinatorial distribution. The signal events are required to lie within the range $5.270\ \text{GeV}/c^2 < m_{\text{ES}} < 5.288\ \text{GeV}/c^2$. This reconstruction procedure results in a yield of approximately 2500 (2000) correctly reconstructed $B^{\pm}$ (B^0) candidates per fb^{-1} of data.

Because the two B mesons are produced with very little momentum in the CM frame, $B\bar{B}$ events typically produce a more isotropic distribution of particles in the detector than nonresonant ("continuum") backgrounds. Such backgrounds ($e^+e^- \to f\bar{f}$, where f represents u, d, s, c or any charged lepton) are suppressed by requiring $R_2 < 0.5$, where R_2 is the ratio of the second to the zeroth Fox-Wolfram moment [22] computed using all charged and neutral particles in the event. Further suppression is achieved by requiring $|\cos\theta_T| < 0.90$, where θ_T is the angle between two thrust axes in the CM frame, the first computed using the particles from the B_{tag}, and the second using all other particles in the event.

All particles that are not used in the B_{tag} reconstruction are considered candidates to be included in the reconstruction of the signal B meson. Since the CM energy is precisely known, reconstruction of the B_{tag} fully determines the B_{signal} 4-vector. This permits the 2-body kinematics of the signal decays to be exploited. In particular, these decays are expected to contain an electron or a muon with a momentum p^*, in the B_{signal} rest frame, of about $2.64\ \text{GeV}/c$ $(2.34\ \text{GeV}/c)$ for the $B^+ \to \ell^+\nu$ ($B^0 \to \ell^+\tau^-$) channels, very close to the kinematic endpoint for B decays.

Signal candidate events are initially selected by requiring the highest momentum track in the event (excluding tracks from the B_{tag} reconstruction) to have a momentum of $1.7\ \text{GeV}/c < p^* < 3.0\ \text{GeV}/c$ and to satisfy particle identification (PID) criteria for either an electron or a muon. In events with a charged B_{tag}, the charge of the track is required to be opposite that of the B_{tag}, while for a neutral B_{tag} the high-p^* lepton is permitted to have either positive or negative charge.

Once the B_{tag} and the signal lepton candidate are identified, $B^+ \to \ell^+\nu$ events should ideally have no other particles in the detector, while $B^0 \to \ell^+\tau^-$ events should additionally contain only the τ^- decay daughters. For the latter, the τ-rest frame is calculated from the observed signal lepton, assuming the nominal energy and momentum of the τ^- for a 2-body B^0 decay. The six τ decay modes considered are listed in Table I. The second highest momentum track in the event (again, excluding B_{tag} reconstruction) is assumed to be a τ daughter, and is required to have a charge opposite to the primary signal lepton. If this track satisfies electron or muon PID, the event is considered to be a leptonic τ decay. Otherwise, the track is assumed to be a pion and the quantity ΔE_τ is calculated

TABLE I. The τ decays considered are listed with their branching fractions, in percent [23].

τ decay mode	Branching Fraction
$e^-\bar{\nu}_e\nu_\tau$	17.84 ± 0.05
$\mu^-\bar{\nu}_\mu\nu_\tau$	17.36 ± 0.05
$\pi^-\nu_\tau$	10.90 ± 0.07
$\pi^-\pi^0\nu_\tau$	25.50 ± 0.10
$\pi^-\pi^0\pi^0\nu_\tau$	9.25 ± 0.12
$\pi^-\pi^-\pi^+\nu_\tau$	9.33 ± 0.08

for the hadronic decay modes listed in Table I. $\Delta E_\tau = \sum E_{\pi^-,\pi^0} + p_\nu - m_\tau$, where $m_\tau = 1.777\ \text{GeV}/c^2$, the sum is over the τ daughter candidates, the momentum of the neutrino is $p_\nu = |\sum \vec{p}_{\pi^-,\pi^0}|$, and all quantities are measured in the τ^- rest frame. We assign the decay mode for which $|\Delta E_\tau|$ is smallest, requiring additional conditions for the decay modes that proceed through the intermediate resonances $\rho^- \to \pi^-\pi^0$, $a_1^- \to \pi^-\pi^0\pi^0$, and $a_1^- \to \pi^-\pi^-\pi^+$. We calculate the quantity $\cos\theta_{\tau-\rho} = (2E_\tau E_\rho - m_\tau^2 - m_\rho^2)/(2|\vec{p}_\tau||\vec{p}_\rho|)$, where $(E_\tau, \vec{p}_\tau)$ and $(E_\rho, \vec{p}_\rho)$ are the four-momenta in the B_{signal} frame, and m_τ and m_ρ are the masses of the τ and ρ. For a correctly reconstructed ρ, this quantity peaks near unity. If the candidate does not satisfy $\cos\theta_{\tau-\rho} > 0.70$ the mode with the next smallest $|\Delta E_\tau|$ (if one is present) is selected instead. Analogous quantities are calculated for the $\tau^- \to \pi^-\pi^0\pi^0\nu_\tau$ and $\tau^- \to \pi^-\pi^-\pi^+\nu_\tau$ modes, but with an $a_1^\pm$ instead of a $\rho^\pm$. The requirements of $\cos\theta_{\tau-a_1} > 0.45$ and $\cos\theta_{\tau-a_1} > 0.35$ are used for the two cases, respectively. There are no additional requirements on the ρ or a_1.

Additional background, for both $B^+ \to \ell^+\nu$ and $B^0 \to \ell^+\tau^-$ decays, can arise from a variety of sources, including beam backgrounds, unassociated hadronic shower fragments, reconstruction artifacts, bremsstrahlung, and photon conversions. We demand that events have no more than two extra charged tracks and six extra neutral clusters, allowing the presence of low energy particles not necessarily associated with the decay of the $\Upsilon(4S)$. Requirements on the missing momentum and extra energy in the event are utilized to ensure that such particles are unimportant for the analysis. Since these requirements are optimized for each signal mode individually, we quote only the values for $B^+ \to \ell^+\nu_\ell$ modes in the text. The signal selection requirements for all signal modes are listed in Table II.

The extra momentum in the event is represented by $\Delta P_{\text{miss}} = |\vec{p}_{\text{miss}} + \sum \vec{p}_{\ell,\pi}|$, where $p_{\ell,\pi}$ are the momenta of the lepton or pion candidate(s) assumed to be recoiling against the neutrinos. The missing momentum is calculated according to $\vec{p}_{\text{miss}} = \vec{p}_{\Upsilon(4S)} - \vec{p}_{B_{\text{tag}}} - \vec{p}_{\text{all}}$, where $\vec{p}_{\text{all}}$ is the momentum of all tracks and clusters left after the B_{tag} reconstruction. ΔP_{miss} is calculated in the rest frame of the parent of the neutrino(s), so that the missing momentum balances the sum of other signal particles' momenta. The signal events are selected by requiring ΔP_{miss} to be less than 0.5 GeV/c.

TABLE II. The signal selection requirements for ΔP_{miss} and E_{extra}, expressed in GeV/c and GeV, respectively, for each decay mode.

Decay mode		ΔP_{miss}	E_{extra}
$B^0 \to \ell^+\tau^-$, $\tau^- \to$	$e^-\bar{\nu}_e\nu_\tau$	<1.2	<0.6
	$\mu^-\bar{\nu}_\mu\nu_\tau$	<1.2	<0.6
	$\pi^-\nu_\tau$	<0.8	<0.6
	$\pi^-\pi^0\nu_\tau$	<0.9	<0.6
	$\pi^-\pi^0\pi^0\nu_\tau$	<1.0	<0.7
	$\pi^-\pi^-\pi^+\nu_\tau$	<1.0	<0.8
$B^+ \to \ell^+\nu$		<0.5	<1.0

For $B^+ \to \ell^+\nu$ modes we also consider the direction of the missing momentum $\cos\theta_{p_{\text{miss}}} = p_{z\text{miss}}/p_{\text{miss}}$, where the subscript z indicates the component of the momentum in the direction parallel to the beam pipe, as measured in the $\Upsilon(4S)$ CM frame. The requirement $-0.76 < \cos\theta_{p_{\text{miss}}} < 0.92$ is determined by the geometry of the detector; events where p_{miss} points outside of the detector acceptance in the forward or backward direction are excluded.

The quantity $E_{\text{extra}} = \sum E_{\text{track}} + \sum E_{\text{cluster}} - E_{\ell^+} - \sum E_{\ell^-,\pi^-,\pi^0}$ describes the amount of energy recorded by the detector that is not accounted for by the high momentum lepton and τ^- daughters (in the case of $B^0 \to \ell^+\tau^-$). The clusters and tracks associated with the reconstruction of B_{tag} are excluded from the sums, and only clusters with energy more than 50 MeV in the CM frame are considered. We require E_{extra} to be less than 1.0 GeV in the CM frame. The signal and background distributions for E_{extra} are shown in Fig. 1.

The signal yields are extracted from unbinned maximum likelihood fits to the signal lepton momentum distributions, as measured in the B_{signal} frame. The signal and background MC distributions are fitted by phenomenological probability density functions (PDF). The signal distributions are modeled with Crystal Ball functions [24] to account for the energy loss due to unreconstructed bremsstrahlung photons. The $B^+ \to \ell^+\nu$ background is modeled with an exponential decay and a Gaussian distribution, while the $B^0 \to \ell^+\tau^-$ background is modeled with a double Gaussian distribution. The PDF parameters are determined from simulated events. The fit is performed using the following likelihood function:

$$\mathcal{L}(n_s, n_b) = \frac{e^{-(n_s+n_b)}}{N!} \prod_{i=1}^{N} [n_s f_s(i) + n_b f_b(i)], \qquad (2)$$

where N is the total number of events in the fit region, $f_s(i)$ and $f_b(i)$ are the PDFs for the signal and background, and n_b and n_s are the number of background and signal events. All parameters of the signal and background PDFs remain fixed, while n_s and n_b are allowed to float. The fits are restricted to the ranges in the lepton momenta shown in Fig. 2.

The 90% confidence level (C.L.) upper limit on the branching fraction $\mathcal{B}$ is determined by solving for $\mathcal{B}^{90\%}$ in $0.90 = \int_0^{\mathcal{B}^{90\%}} \mathcal{L}(\mathcal{B})d\mathcal{B} / \int_0^\infty \mathcal{L}(\mathcal{B})d\mathcal{B}$ for events lying in the signal regions of $2.40\ \text{GeV}/c < p^* < 2.75\ \text{GeV}/c$ for $B^+ \to \ell^+\nu$ and $2.20\ \text{GeV}/c < p^* < 2.42\ \text{GeV}/c$ for $B^0 \to \ell^+\tau^-$. $\mathcal{B}$ is related to the signal yield n_s^* through a substitution $n_s^* = \epsilon_{\text{tot}} \times 2 \times N_{B\bar{B}} \times \mathcal{B}$, where ϵ_{tot} is the

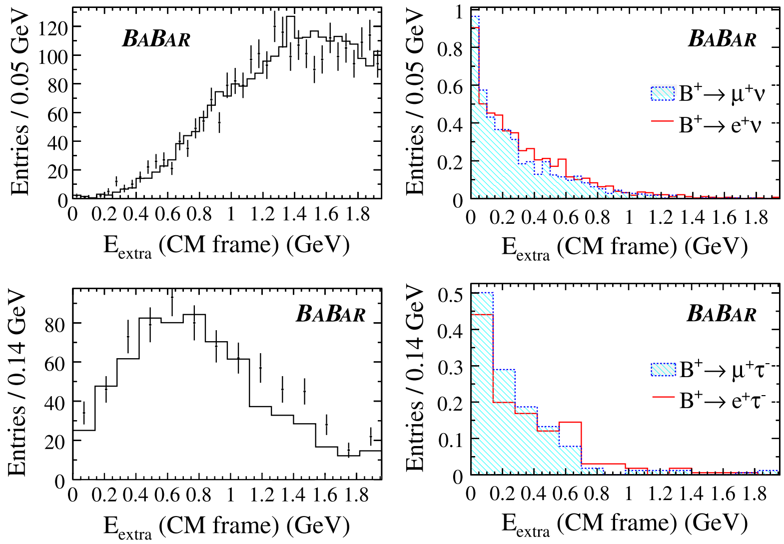

FIG. 1 (color online). E_{extra} distributions for the background simulation and data (left) and the signal (right) after all other selection criteria have been applied. The upper plots are for $B^+ \to \ell^+ \nu$ modes and the lower plots are for $B^0 \to \ell^+ \tau^-$ modes. The background distributions show electron and muon modes together, as they are nearly identical. The background is almost completely dominated by $B\bar{B}$ events. The signal modes are shown with a branching fraction of 10^{-5}.

total signal selection efficiency and $N_{B\bar{B}}$ is the number of B^+B^- or $B^0\bar{B}^0$ pairs in the data sample. The signal selection efficiencies, expected number of background events and fit results are given in Table III. The number of signal events given by the fits is consistent with zero for all decay modes. The uncertainties in Table III are statistical except for those shown for $\mathcal{B}$ which are the statistical and systematic uncertainties added in quadrature.

The systematic uncertainties arising from the fitting procedure are studied by repeating the procedure on additional simulated samples, generated according to the PDFs, with varying number of signal events. Systematic effects are studied by repeating the procedure with PDF parameters varied by their uncertainties. For the case of zero signal events, we find negligible effects on the branching fraction values, and take the standard deviation of n_s and n_b from their expected values in the fits as systematic uncertainties.

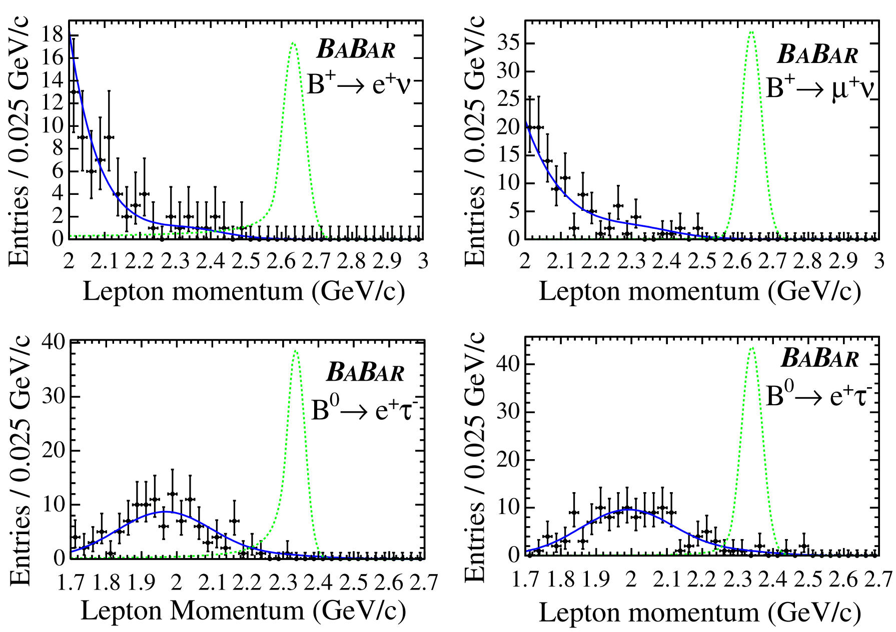

FIG. 2 (color online). The unbinned maximum likelihood fits on the lepton momentum. The dashed line, representing the signal PDF with an arbitrary scaling, indicates where the signal is expected.

TABLE III. Signal selection efficiency ϵ_{tot} determined from MC, the fitted numbers of signal and background events in the signal regions n_s^* and n_b^*, and the branching fractions $\mathcal{B}$. The uncertainties for $\mathcal{B}$ include statistical and systematic terms. The uncertainties for the other quantities are statistical only.

	Signal Mode			
	$e^+\nu$	$\mu^+\nu$	$e^+\tau^-$	$\mu^+\tau^-$
$\epsilon_{\text{tot}} \times 10^5$	135 ± 4	120 ± 4	32 ± 2	27 ± 2
n_b^* MC	2.66 ± 0.13	5.74 ± 0.25	8.69 ± 0.27	12.14 ± 0.45
n_b^*	2.67 ± 0.19	5.67 ± 0.34	9.35 ± 0.35	13.03 ± 0.31
n_s^*	-0.07 ± 0.03	-0.11 ± 0.05	0.02 ± 0.01	0.01 ± 0.01
$\mathcal{B} \times 10^{-6}$	$-0.1^{+2.6}_{-1.7}$	$-0.2^{+2.7}_{-1.8}$	0^{+15}_{-10}	0^{+11}_{-7}
$\mathcal{B}^{90\%\ \text{C.L.}}$	5.2×10^{-6}	5.6×10^{-6}	2.8×10^{-5}	2.2×10^{-5}

We find the fits to be well behaved and having no significant sources of bias, introducing no additional uncertainties. Total uncertainties associated with the fitting procedure are listed in Table III for each decay mode.

The discrepancies between simulation and data are treated as detailed in the following paragraphs. The number of correctly reconstructed B_{tag} events in the m_{ES} signal region is compared between simulation and data. The m_{ES} distributions for simulation and data are fitted with a combination of ARGUS [25] and Crystal Ball functions, allowing the number of m_{ES} peaking events to be estimated by integrating the peaking component between 5.270 GeV$/c^2$ and 5.288 GeV$/c^2$. We find the simulation to underestimate the number of events with a good B_{tag} and scale the signal selection efficiency by a factor of 1.11 ± 0.06 (1.05 ± 0.06) for events with a neutral (charged) B_{tag}.

In addition, the PID efficiencies in simulation are corrected for the 2%–5% lower efficiencies in data. We assign associated uncertainties of about 2% for high momentum particles (signal lepton), and about 5% for tau daughters. The misidentification rate of leptons and pions is found to be negligible in the simulated samples, after all selection criteria are applied. An uncertainty in the tracking algorithm introduces an additional 0.8% systematic uncertainty for each charged track present in any given signal mode (e.g. 1.6% for $B^0 \to \ell^+\tau^-$, $\tau^- \to \pi^-\nu_\tau$). The uncertainties for $B^0 \to \ell^+\tau^-$ modes are calculated as weighted averages of all τ^- decay modes.

TABLE IV. The sources and magnitudes of systematic uncertainties, in percent.

	Signal Mode			
Uncertainty source	$e + \tau -$	$\mu + \tau -$	$e^+\nu$	$\mu^+\nu$
Signal Fit	5.6	10.6	4.3	8.2
Background Fit	3.9	3.1	5.1	7.8
B_{tag} efficiency	6.4	6.4	5.8	5.8
PID efficiency	5.3	5.8	1.0	2.0
MC Statistics	8.6	7.4	3.0	2.8
Tracking efficiency	1.7	1.7	0.8	0.8
$N_{B\bar{B}}$	1.1	1.1	1.1	1.1

Table IV lists the sources and the magnitudes of the uncertainties with their effect on $\mathcal{B}$. The uncertainties are incorporated into the final results by varying the branching fraction assumption by its uncertainty when integrating $\mathcal{L}$ for the 90% C.L. upper limit.

We have presented searches for the rare leptonic decays $B^+ \to \ell^+\nu$ and $B^0 \to \ell^\pm\tau^\mp$, where $\ell = e$, μ, using a novel hadronic tag reconstruction technique. We find no evidence of signal in any of the decay modes in a data sample of approximately 378×10^6 $B\bar{B}$ pairs (342 fb^{-1}), and set the branching fraction upper limits at $\mathcal{B}(B^+ \to e^+\nu) < 5.2 \times 10^{-6}$, $\mathcal{B}(B^+ \to \mu^+\nu) < 5.6 \times 10^{-6}$, $\mathcal{B}(B^0 \to e^+\tau^-) < 2.8 \times 10^{-5}$, and $\mathcal{B}(B^0 \to \mu^+\tau^-) < 2.2 \times 10^{-5}$, at 90% confidence level. While these upper limits on $\mathcal{B}(B^+ \to e^+\nu)$ and $\mathcal{B}(B^+ \to \mu^+\nu)$ complement the more stringent limits available from inclusive studies [14,16], the $B^0 \to e^+\tau^-$ and $B^0 \to \mu^+\tau^-$ results are the most stringent published upper limits available.

We are grateful for the extraordinary contributions of our PEP-II colleagues in achieving the excellent luminosity and machine conditions that have made this work possible. The success of this project also relies critically on the expertise and dedication of the computing organizations that support *BABAR*. The collaborating institutions wish to thank SLAC for its support and the kind hospitality extended to them. This work is supported by the US Department of Energy and National Science Foundation, the Natural Sciences and Engineering Research Council (Canada), the Commissariat à l'Energie Atomique and Institut National de Physique Nucléaire et de Physique des Particules (France), the Bundesministerium für Bildung und Forschung and Deutsche Forschungsgemeinschaft (Germany), the Istituto Nazionale di Fisica Nucleare (Italy), the Foundation for Fundamental Research on Matter (The Netherlands), the Research Council of Norway, the Ministry of Science and Technology of the Russian Federation, Ministerio de Educación y Ciencia (Spain), and the Science and Technology Facilities Council (United Kingdom). Individuals have received support from the Marie-Curie IEF program (European Union) and the A. P. Sloan Foundation.

[1] Throughout this paper, decay modes imply also their charge conjugates.
[2] Super B Collaboration, arXiv:0709.0451v2.
[3] W.-S. Hou, Phys. Rev. D **48**, 2342 (1993).
[4] A. Dedes, J. Ellis, and M. Raidal, Phys. Lett. B **549**, 159 (2002).
[5] D. Silverman and H. Yao, Phys. Rev. D **38**, 214 (1988).
[6] N. Cabbibo, Phys. Rev. Lett. **10**, 531 (1963); M. Kobayashi and T. Maskawa, Prog. Theor. Phys. **49**, 652 (1973).
[7] E. Barberio *et al.* (Heavy Flavor Averaging Group), arXiv: hep-ex/0603003.
[8] A. Gray *et al.* (HPQCD Collaboration), Phys. Rev. Lett. **95**, 212001 (2005).
[9] B. Aubert *et al.* (*BABAR* Collaboration), Phys. Rev. D **76**, 052002 (2007).
[10] K. Ikado *et al.* (BELLE Collaboration), Phys. Rev. Lett. **97**, 251802 (2006).
[11] A. Masiero and P. Paradisi, J. Phys. Conf. Ser. **53**, 248 (2006).
[12] M. Artuso *et al.* (CLEO Collaboration), Phys. Rev. Lett. **99**, 071802 (2007); K. M. Ecklund *et al.* (CLEO Collaboration), Phys. Rev. Lett. **100**, 161801 (2008).
[13] K. Abe *et al.* (Belle Collaboration), arXiv:0709.1340 [Phys. Rev. Lett. (to be published)].
[14] N. Satoyama *et al.* (BELLE Collaboration), Phys. Lett. B **647**, 67 (2007).
[15] M. Artuso *et al.* (CLEO Collaboration), Phys. Rev. Lett. **75**, 785 (1995).
[16] B. Aubert *et al.* (*BABAR* Collaboration), Phys. Rev. Lett. **92**, 221803 (2004).
[17] A. Bornheim *et al.* (CLEO Collaboration), Phys. Rev. Lett. **93**, 241802 (2004).
[18] S. Agostinelli *et al.*, Nucl. Instrum. Methods Phys. Res., Sect. A **506**, 250 (2003).
[19] B. Aubert *et al.* (*BABAR* Collaboration), Nucl. Instrum. Methods Phys. Res., Sect. A **479**, 1 (2002).
[20] B. Barish *et al.* (CLEO Collaboration), Phys. Rev. Lett. **76**, 1570 (1996).
[21] B. Aubert *et al.* (*BABAR* Collaboration), Phys. Rev. Lett. **92**, 071802 (2004).
[22] G. C. Fox and S. Wolfram, Phys. Rev. Lett. **41**, 1581 (1978).
[23] W.-M. Yao *et al.* (2006 Review of Particle Physics), J. Phys. G **33**, 1 (2006).
[24] J. E. Gaiser *et al.* (Crystal Ball Collaboration), Report No. SLAC-R-255, 1982.
[25] H. Albrecht *et al.* (ARGUS Collaboration), Phys. Lett. B **241**, 278 (1990).